Supercontinuum generation in planar glass membrane fibers: comparison with bulk media

M. Kolesik,[1,2,*] D. Faccio,[3,4] E. M. Wright,[1] P. Di Trapani,[3,4,5] and J. V. Moloney[1,2]

[1]College of Optical Sciences, University of Arizona, Tucson, Arizona 85721, USA
[2]Arizona Center for Mathematical Sciences, University of Arizona, Tucson, Arizona 85721, USA
[3]CNISM and Department of Physics and Mathematics, University of Insubria, Como 22100, Italy
[4]Virtual Institute for Nonlinear Optics, Centro di Cultura Scientifica Alessandro Volta, Como 22100, Italy
[5]Department of Quantum Electronics, Vilnius University, Vilnius LT-01222, Lithuania
*Corresponding author: kolesik@acms.arizona.edu

Received September 19, 2008; revised October 31, 2008; accepted November 16, 2008;
posted December 16, 2008 (Doc. ID 101799); published January 26, 2009

Planar glass membrane fibers (PGMFs) are of current interest owing to the fact that they combine the interesting dispersive properties of fibers with diffraction in one unbound transverse dimension. We study supercontinuum (SC) spectra generated in PGMFs and show that the underlying dynamics has similarities to bulk medium. At the same time, the rich dispersion properties of PGMFs open up new possibilities, including SC spectral shapes that do not occur in natural bulk media. In all cases, the SC spectra in PGMFs can be interpreted in detail using the effective-three-wave-mixing model originally developed for bulk media. © 2009 Optical Society of America

OCIS codes: 320.2250, 320.5550, 190.5940, 190.7110, 190.5530.

High-power laser pulses propagating in nonlinear Kerr media broaden their spectrum through self-phase modulation (SPM). If the intensities are high enough SPM broadening may be enhanced by a number of effects leading to a spectacular spectral reshaping, commonly known as white light or supercontinuum (SC) generation. SC is common to all media, gaseous, liquid, and condensed, and has been observed in both optical fibers and bulk geometries [1]. In bulk media SC is often associated with filamentation, i.e., self-focusing of the input beam and the formation of a tightly focused high-intensity peak that propagates subdiffractively over many Rayleigh lengths [2,3]. SC efficiency in this regime is not strictly connected with the sign of the group-velocity dispersion (GVD). On the other hand, in fiber geometries it is well known that SC is greatly enhanced when the pump is located close to the zero GVD wavelength, thus leading to the formation of a soliton that in certain regimes will undergo fission [4], stimulated Raman scattering with a self-induced frequency shift and, notably for the present work, formation of spectrally shifted peaks known as dispersive waves [5,6], also often termed Cerenkov [7] or resonant radiation [4].

In this Letter we explore SC generation in (ideal) planar glass membrane fibers (PGMFs) and compare it to the known properties of SC in bulk media. The PGMF was recently introduced and has a core in the shape of an extremely thin but very wide planar waveguide [8]. On the one hand, the dispersion landscape of a submicrometer silica PGMF shares many features with that for silica nanowires. In particular, depending on the chosen membrane thickness and on the light polarization, both normal and anomalous GVD regimes can be explored even at the same wavelength. On the other hand, constant-thickness PGMF fibers only confine light in a single transverse direction, so in the unbound direction they exhibit one-dimensional diffraction. We will show that this additional diffractive degree of freedom means that the SC from PGMFs can be understood in a manner similar to bulk media.

In comparing SC generation in PGMFs to bulk media, some qualitative differences arise owing to the degree of collapse in each case. First, it is well known that critical collapse requires the product of the nonlinearity order and the dimension be equal to four. Thus, strictly speaking, in PGMFs with one transverse dimension there is no collapse in a Kerr medium, just focusing to a spatial solitary wave. For ultrashort pulses normal GVD can lead to temporal pulse splitting, whereas anomalous GVD can, in principle, lead to simultaneous collapse in space and time, but if the dispersion length differs from the diffraction length then some compression occurs, but this is not a true collapse (in the examples that follow, diffraction lengths are typically less than 1 cm, while dispersion lengths are between 1 and 2 cm). This "collapse inhibition" makes SC generation in PGMFs more difficult relative to bulk media.

To proceed, we first give a brief overview of the effective-three-wave-mixing (ETWM) model for SC generation, which we shall use to interpret the SC spectra [9,10]. According to the ETWM paradigm [9], white-light generation in a bulk medium originates from the creation of a nonlinear optical response driven by strongly localized optical wave packets, owing to the combined effects of self-focusing in two transverse dimensions and GVD, and subsequent scattering of the wave packets from the nonlinear response leading to SC generation. The efficiency of the ETWM process is dictated by a phase-matching relation [10]. Denoting by $K(\omega,k_\perp)$ the propagation constant of a plane wave with angular frequency ω and transverse wavenumber $k_\perp$, then for a medium with

a linear dielectric permittivity $\epsilon(\omega)$ we have $K(\omega,k_\perp)\equiv\sqrt{k^2-k_\perp^2}$, with $k=\omega\sqrt{\epsilon(\omega)}/c$ and the ETWM phase-matching relation reads as

$$K(\omega,k_\perp)-K(\omega_p,0)-\left(\frac{\omega-\omega_p}{v_p}\right)\approx 0, \qquad (1)$$

where ω_p is the wave-packet center frequency and v_p is the velocity of the peak of the nonlinear response. Equation (1) determines the loci of scattered transverse wavenumbers and frequencies in the $(\omega,k_\perp)$ plane that will be most significantly populated by the ETWM process, and thus defines the region(s) where power will be concentrated in the far-field SC spectrum.

We want to test if the above picture applies to PGMFs, where the transverse wavenumber vector $k_\perp$ has a single (in-plane) component, while the field remains confined to the bound mode in the out-of-plane direction. The frequency-dependent propagation constant $k(\omega)$ entering Eq. (1) is then replaced by the propagation constant of this guided mode, and the phase-matching condition thus reflects the dispersion properties of the fiber. We remark that the peak velocity v_p in Eq. (1) does not necessarily coincide with the group velocity $d\omega/dk$ at ω_p. This difference is connected with the presence of transverse dimensions along which diffraction, and thus space–time coupling, may occur.

We have performed femtosecond pulse propagation simulations in silica PGMF using the unidirectional pulse propagation equation [11] solver with precalculated, frequency-dependent modal properties. We performed a range of simulations at various wavelengths and waveguide thicknesses. Here we present illustrative examples of our results for a center wavelength of 800 nm and two waveguide core thicknesses chosen to illustrate the rich variety of SC spectra that can arise. The silica nonlinear properties were modeled using an instantaneous Kerr effect and a 20% contribution from the stimulated Raman effect approximated by a single damped oscillator. Comparative examples of supercontinua generated in water are also shown to emphasize the bulklike character of the SC generation dynamics in PGMFs.

Example 1. We start with an example showing the generation of X waves in a PGMF for a wavelength in the normal GVD regime. In particular, we consider a 600-nm-thick PGMF with a TE-polarized, 60 fs incident pulse that is collimated to a 50 μm waist at 1 TW/cm^2 peak intensity. At 800 nm wavelength, the initial pulse propagates in the normal GVD regime and undergoes self-focusing (without collapse) that is subsequently halted by a pulse splitting event quite similar to those that occur in condensed bulk media. The two split-off daughter pulses, which develop intensities about three times the input, both act as localized wave packets that produce different components of the generated SC spectrum shown in Fig. 1. To test if the ETWM picture can be used to interpret the PGMF spectrum, we have extracted from the simulation data the propagation velocities v_p of the two main peaks in the medium nonlinear response,

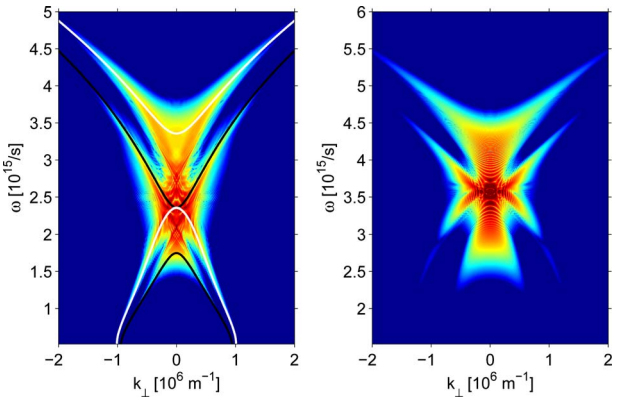

Fig. 1. (Color online) Angularly resolved (log scale) spectrum from a 600-nm-thick silica PGMF for a TE-polarized pulse of 60 fs duration and center wavelength 800 nm, resulting in an X-shaped spectrum. For comparison, the right panel shows supercontinuum generated in water ($\lambda=527$ nm, 80 fs, 4 μJ, 3 cm distance).

(see [9] for details of the procedure) and used these in Eq. (1) together with the propagation constant $k(\omega)$ calculated for the TE mode of the glass membrane. Indeed, the phase-matching relation Eq. (1) accurately predicts the location of spectral power in the $(\omega,k_\perp)$ plane: The white and black curves in Fig. 1 show the phase-matched loci corresponding to the respective trailing and leading split-off peak velocities. This scenario is qualitatively equivalent to the SC generation in water (see Fig. 1).

Example 2. Our second example involves SC generation in a PGMF but now for a center wavelength of 800 nm in the anomalous GVD regime. Figure 2 shows a spectrum for a 1-μm-thick PGMF and a TM-polarized input pulse of 30 fs duration. Again, the phase-matching relation Eq. (1) accurately predicts the location of spectral power in the $(\omega,k_\perp)$ plane, the black lines showing the phase-matched loci corresponding to the pulse velocity v_p as deduced from the nonlinear response obtained from the simulations. We note that this fishlike-shaped spectrum was previously studied theoretically for PGMFs in [12] but

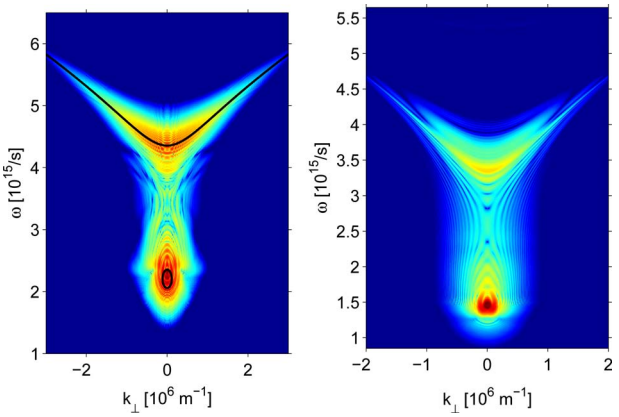

Fig. 2. (Color online) Angularly resolved spectrum generated in a 1000-nm-thick silica PGMF for a TM-polarized pulse of 30 fs duration and center wavelength 800 nm, resulting in a fishlike-shaped spectrum. For comparison, a similar spectrum generated in water ($\lambda=1300$ nm, 80 fs, 8 μJ, 1 cm distance) is shown in the right panel.

that the predicted locus of the resonant radiation was shifted with respect to numerical simulations. This shift appeared owing to the use of the group velocity v_s calculated from the material dispersion relations in the phase-matching relation: Owing to space-time coupling occurring in the unbound transverse dimension of the PGMF, the group velocity is slightly different from v_s so that the peak velocity v_p should be used, as implied by Eq. (1), and shown in Fig. 2.

The fishlike shape of the SC spectrum is also characteristic of SC generation in bulk media in the anomalous regime when the phase-matched radiation is scattered into the normal GVD frequency region where it forms the "fish tail." The right panel in Fig. 2 depicts an example for water.

Example 3. Our final example of SC generation in a PGMF has no analogy in naturally occurring bulk media because it relies on the fiberlike dispersion properties of the PGMF. In particular, for SC generated in a fiber using a wavelength situated between two dispersion zeros, a characteristic spectrum arises with a broad spectral peak on each normal-GVD side of the two zeros [13]. Figure 3 shows the analogous situation for a 600-nm-thick PGMF for a TM-polarized input field at 800 nm wavelength. The SC spectrum clearly exhibits low- and high-frequency spectral components that both propagate in the normal GVD regime, and both of them are generated by a single dominant peak that acquires a group velocity very close to that of the input pulse when it reaches its maximal intensity. Once again, the black curve in Fig. 3 demonstrates that it is the velocity v_p of the peak of the nonlinear response that determines where the SC spectrum becomes populated in the $(\omega, k_\perp)$ plane.

In summary, we have shown that PGMFs can show SC spectra both analogous to and distinct from those in bulk media. The similarity between the SC generation dynamics in PGMFs and bulk is due to the unbound dimension in the glass membrane fiber core, and this allows the SC spectra for PGMFs to display features analogous to bulk media. On the other hand, the dispersive properties of the PGMFs allow for new SC spectral features not shared by bulk media. Furthermore, we have shown that the ETWM model previously employed for bulk media can accurately explain the topology of the SC spectra of PGMFs, and the concentrations of the energy in the SC spectra of PGMFs are quantitatively related to the propagation velocities of the nonlinear response peaks driven by the optical pulse.

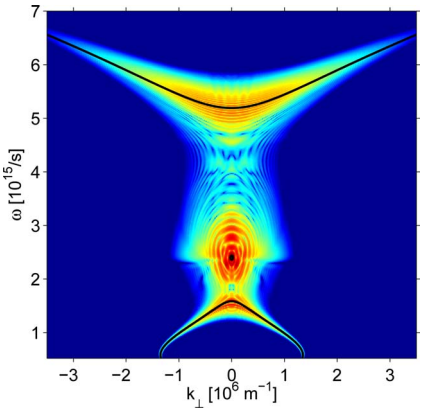

Fig. 3. (Color online) Far-field spectrum generated by a TM-polarized input pulse of 30 fs duration in a 600-nm-thick PGMF, resulting in a spectrum that extends into both the normal and anomalous dispersion regions.

Besides their potential for applications, PGMFs offer new exciting possibilities owing to their unique combination of bulk and fiber properties. The rich, polarization-dependent dispersion landscape, together with a bulklike diffractive degrees of freedom provide us with a whole new "laboratory" to study basic physics of femtosecond pulse dynamics.

This work was supported by Air Force Office of Scientific Research under contract FA9550-07-1-0010. D. Faccio and P. D. Di Trapani acknowledge support from the Consorzio Nazionale Interuniversitario per le Scienze Fisiche della Materia (CNISM), project INNESCO. P. D. Di Trapani acknowledges support from the Marie Curie Chair project STELLA MEXC-CT-2005-025710.

References

1. R. R. Alfano, ed., *The Supercontinuum Laser Source* (Springer-Verlag, 1989).
2. A. Couairon and A. Mysyrowicz, Phys. Rep. **441**, 47 (2007).
3. L. Bergé, S. Skupin, R. Nuter, J. Kasparian, and J. Wolf, Rep. Prog. Phys. **70**, 1633 (2007).
4. J. M. Dudley, G. Genty, and S. Coen, Rev. Mod. Phys. **78**, 1135 (2006).
5. A. V. Husakou and J. Herrmann, Phys. Rev. Lett. **87**, 203901 (2001).
6. J. Herrmann, U. Griebner, N. Zhavoronkov, A. Husakou, D. Nickel, J. C. Knight, W. J. Wadsworth, P. S. J. Russell, and G. Korn, Phys. Rev. Lett. **88**, 173901 (2002).
7. N. Akhmediev and M. Karlsson, Phys. Rev. A **51**, 2602 (1995).
8. N. Y. Joly, T. A. Birks, A. Yulin, J. C. Knight, and P. S. J. Russell, Opt. Lett. **30**, 2469 (2005).
9. M. Kolesik, E. M. Wright, and J. V. Moloney, Opt. Express **13**, 10729 (2005).
10. M. Kolesik, E. M. Wright, and J. V. Moloney, Phys. Rev. Lett. **92**, 253901 (2004).
11. M. Kolesik and J. V. Moloney, Phys. Rev. E **70**, 036604 (2004).
12. A. V. Yulin, D. V. Skryabin, and P. S. J. Russell, Opt. Lett. **30**, 525 (2005).
13. K. M. Hilligsoe, T. Andersen, H. Paulsen, C. Nielsen, K. Molmer, S. Keiding, R. Kristiansen, K. Hansen, and J. J. Larsen, Opt. Express **12**, 1045 (2004).